

## Electronic Supplementary Information

# Multiple 2D crystal structures in bilayered lamellae from direct self-assembly of 3D systems of soft Janus particles

Yu-Wei Sun,<sup>†,‡</sup> Zhan-Wei Li,<sup>\*,†,‡</sup> and Zhao-Yan Sun<sup>\*,†,‡</sup>

<sup>†</sup>*State Key Laboratory of Polymer Physics and Chemistry, Changchun Institute of Applied  
Chemistry, Chinese Academy of Sciences, Changchun 130022, China*

<sup>‡</sup>*University of Science and Technology of China, Hefei, 230026, China*

E-mail: zwli@ciac.ac.cn; zysun@ciac.ac.cn

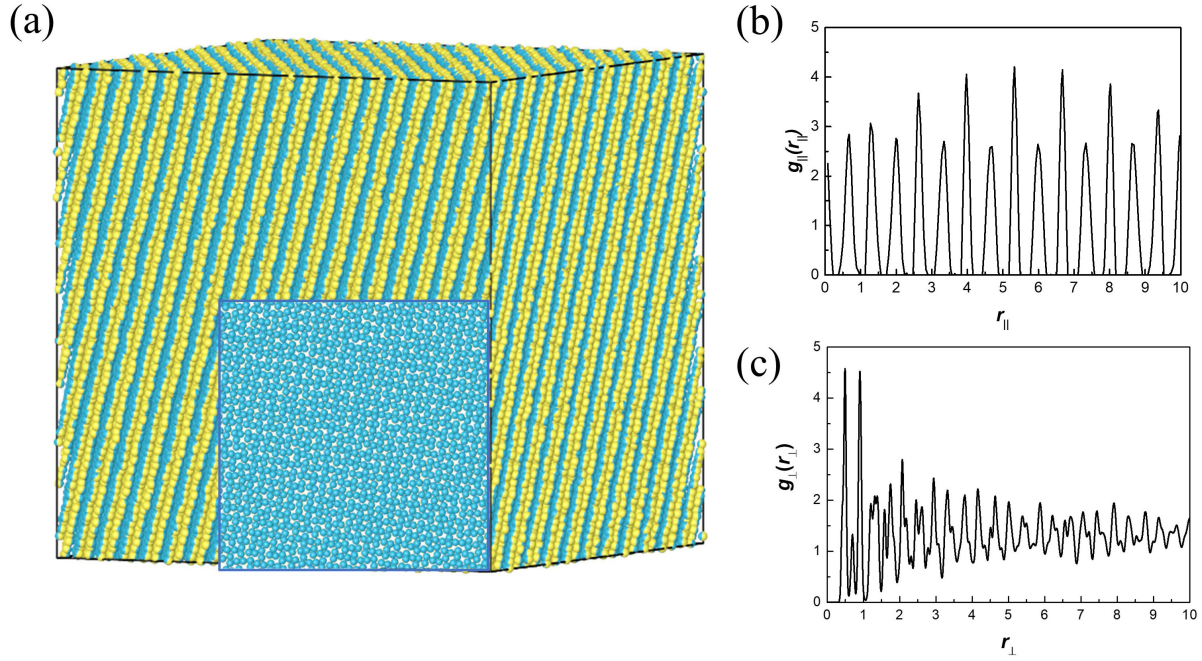


Figure S1: (a) Typical self-assembled bilayered lamellar phase ( $\sigma$  phase within layers) with larger system size of  $1.755 \times 10^5$  particles in a  $30 \times 30 \times 30$  cubic box. (b) The parallel distribution function  $g_{\parallel}(r_{\parallel})$ . (c) The perpendicular radial distribution function  $g_{\perp}(r_{\perp})$ .

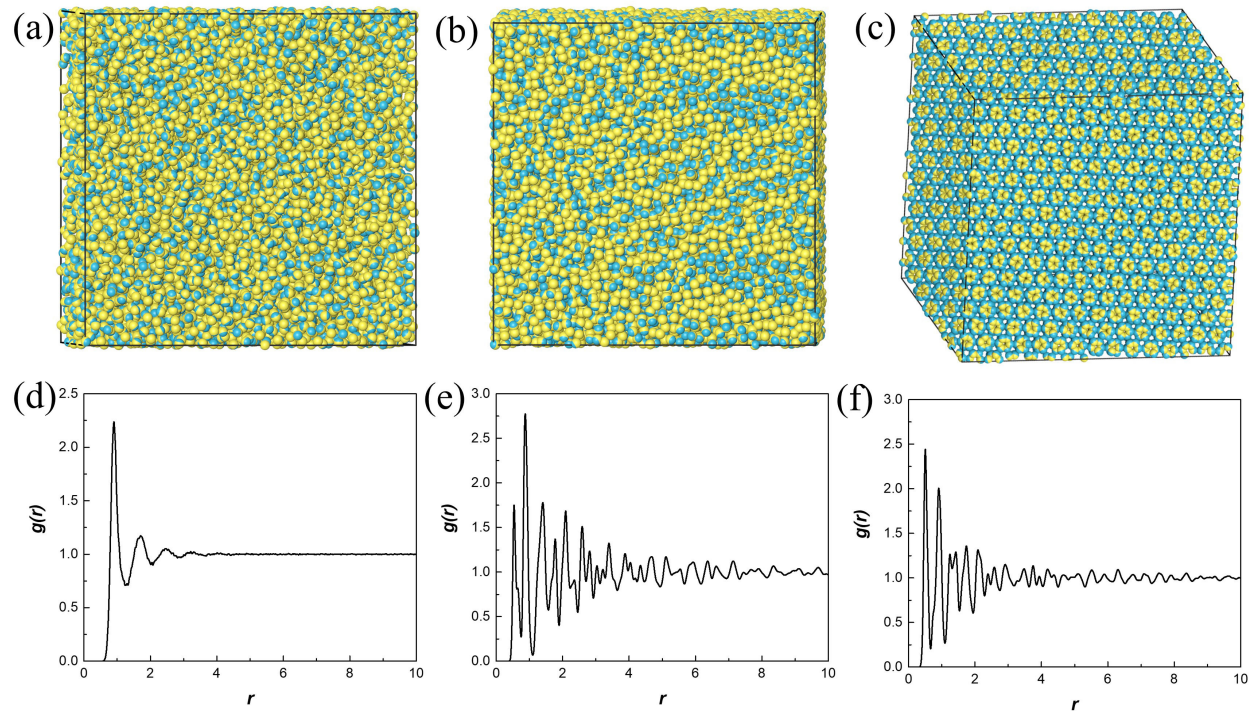


Figure S2: Typical self-assembled structures of soft Janus particles. The typical snapshot of (a) amorphous phase (A), (b) cubic  $Ia\bar{3}d$  phase (CI), (c) columnar phase (C). The radial distribution function of the (d) amorphous phase, (e) cubic  $Ia\bar{3}d$  phase, (f) columnar phase

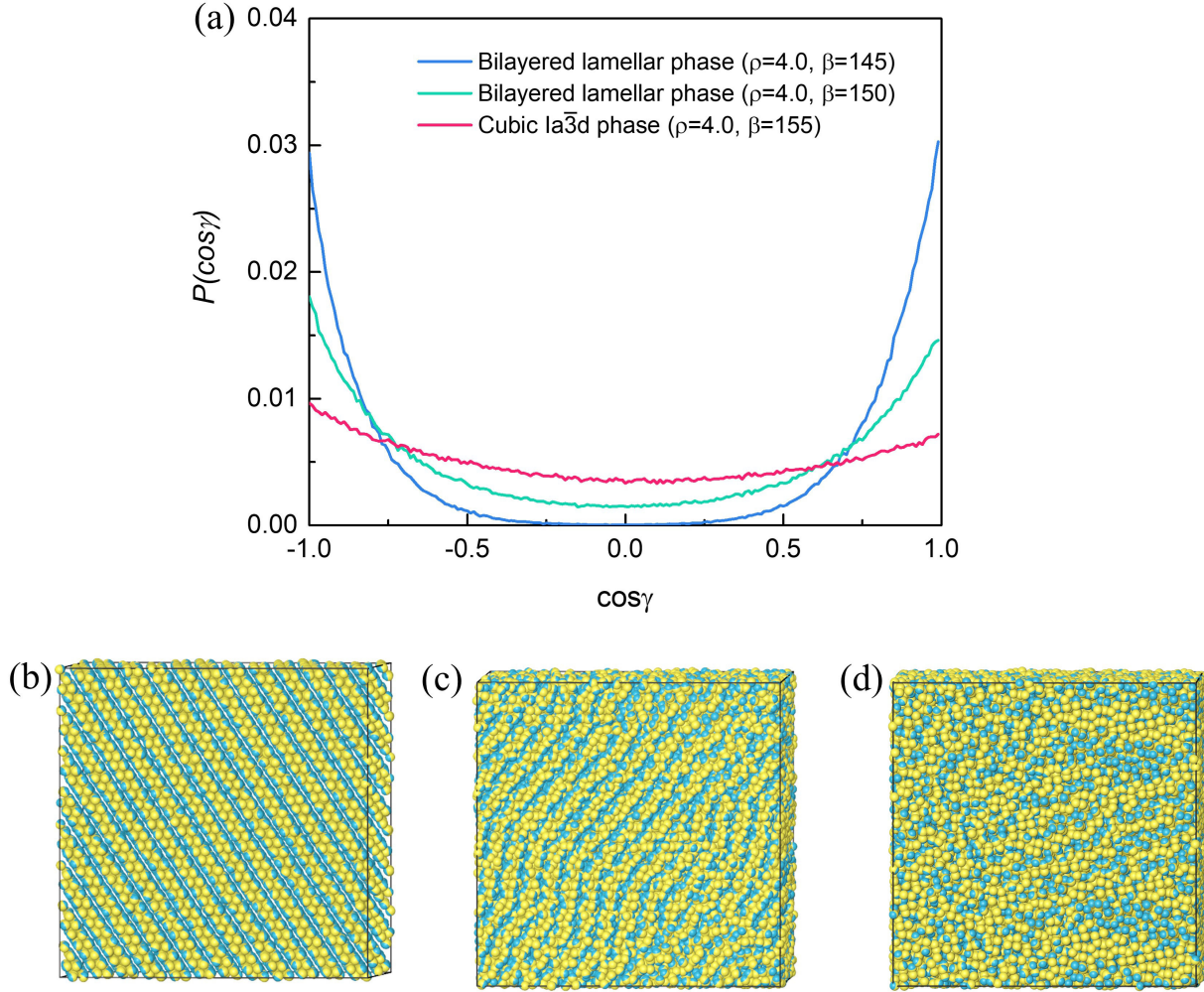


Figure S3: (a) Distribution of the scalar product between the unit vectors of all pairs of contacted SJs<sup>1</sup> ( $\cos \gamma = \mathbf{n}_i \cdot \mathbf{n}_j$ ) for bilayered lamellar phase and cubic  $Ia\bar{3}d$  phase. (b) The snapshot of bilayered lamellar phase ( $\rho = 4.0, \beta = 145^\circ$ ). (c) The snapshot of bilayered lamellar phase ( $\rho = 4.0, \beta = 150^\circ$ ). (d) The snapshot of cubic  $Ia\bar{3}d$  phase ( $\rho = 4.0, \beta = 155^\circ$ ).



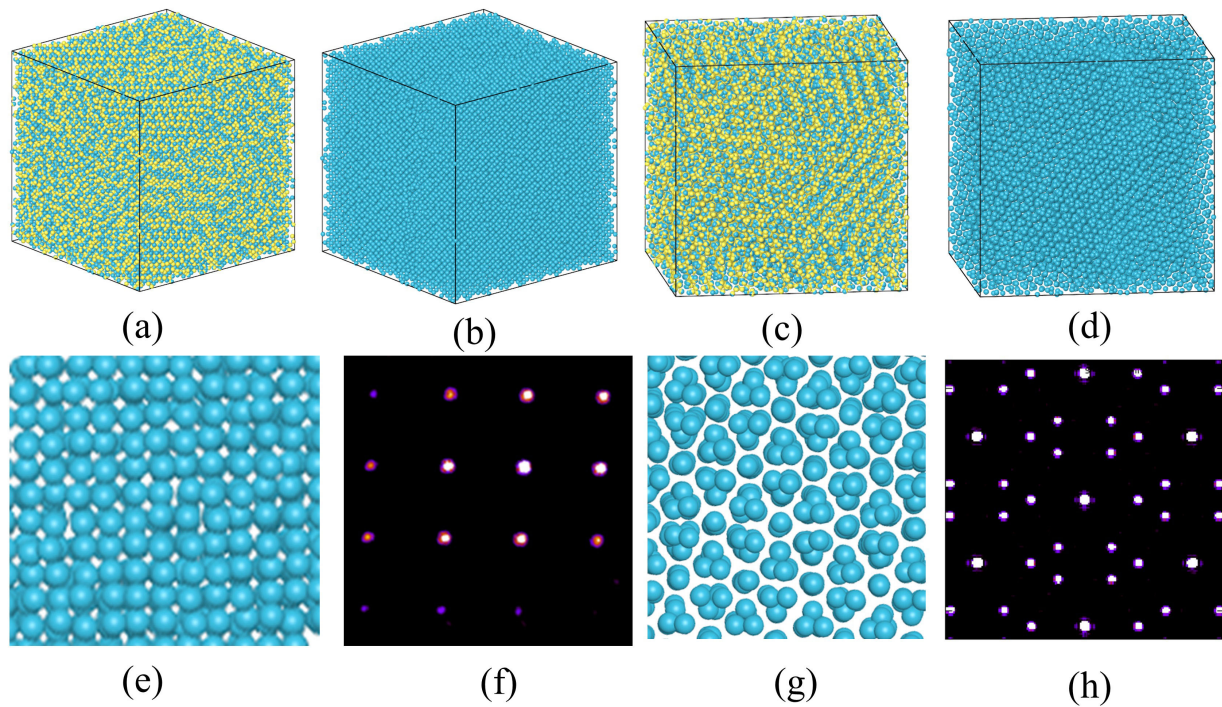


Figure S4: Structural characteristics of cubic  $Ia\bar{3}d$  (CI) phase. (a) cubic  $Ia\bar{3}d$  phase along  $\langle 100 \rangle$  direction, (b) cubic  $Ia\bar{3}d$  phase along  $\langle 100 \rangle$  direction (without showing the patches for clarity), (c) cubic  $Ia\bar{3}d$  phase along  $\langle 111 \rangle$  direction, (d) cubic  $Ia\bar{3}d$  phase along  $\langle 111 \rangle$  direction (without showing the patches for clarity), (e) 2D-projected view of cubic  $Ia\bar{3}d$  phase along  $\langle 100 \rangle$  direction, (f) diffraction patterns of cubic  $Ia\bar{3}d$  phase corresponding to the views of panels e, (g) 2D-projected view of cubic  $Ia\bar{3}d$  phase along  $\langle 111 \rangle$  direction, (h) diffraction patterns of cubic  $Ia\bar{3}d$  phase corresponding to the views of panels h.

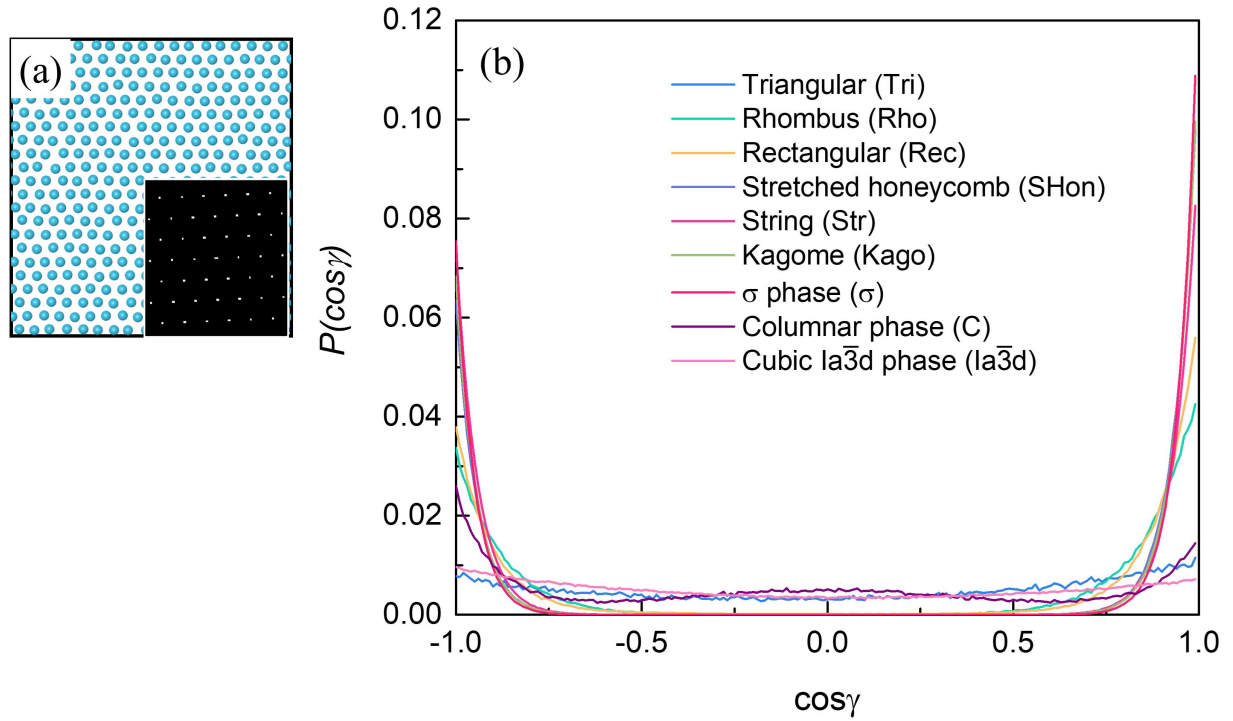


Figure S5: Structural characteristics of self-assembled structures. (a) Typical ordered 2D triangular lattice within layers of bilayered lamellae and corresponding diffraction pattern. (b) Distribution of the scalar product between the unit vectors of all pairs of contacted SJPs ( $\cos \gamma = \mathbf{n}_i \cdot \mathbf{n}_j$ ).

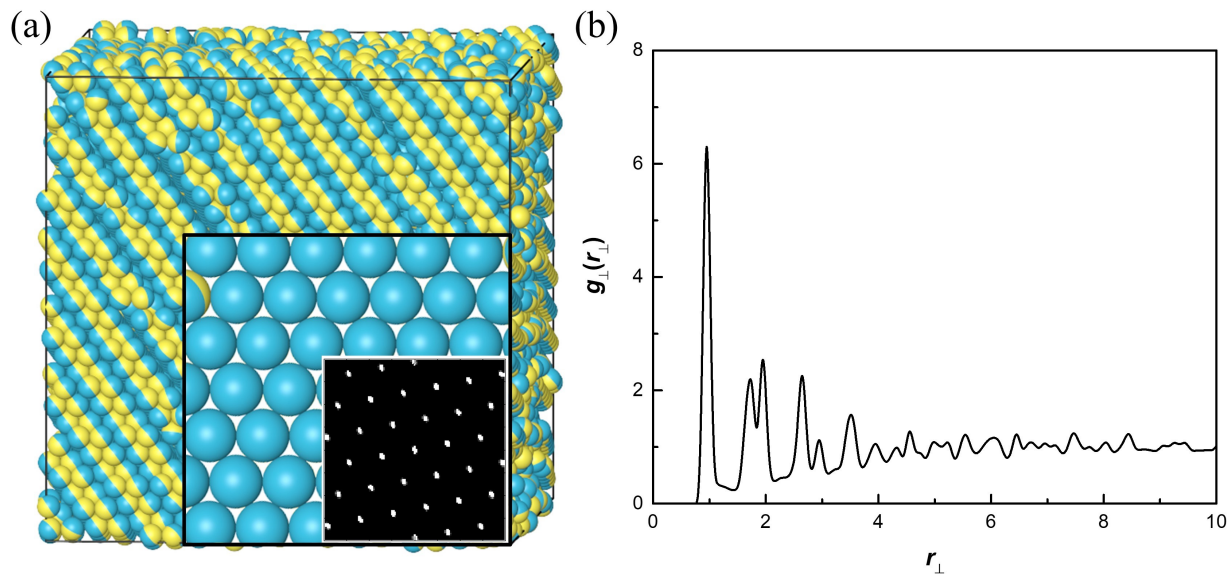


Figure S6: (a) Typical triangular lattice within each layer of self-assembled bilayered lamellae from harder Janus particles with  $\alpha_{ij}^R = 39996$  and the corresponding diffraction pattern. (b) The perpendicular radial distribution function  $g_{\perp}(r_{\perp})$ .

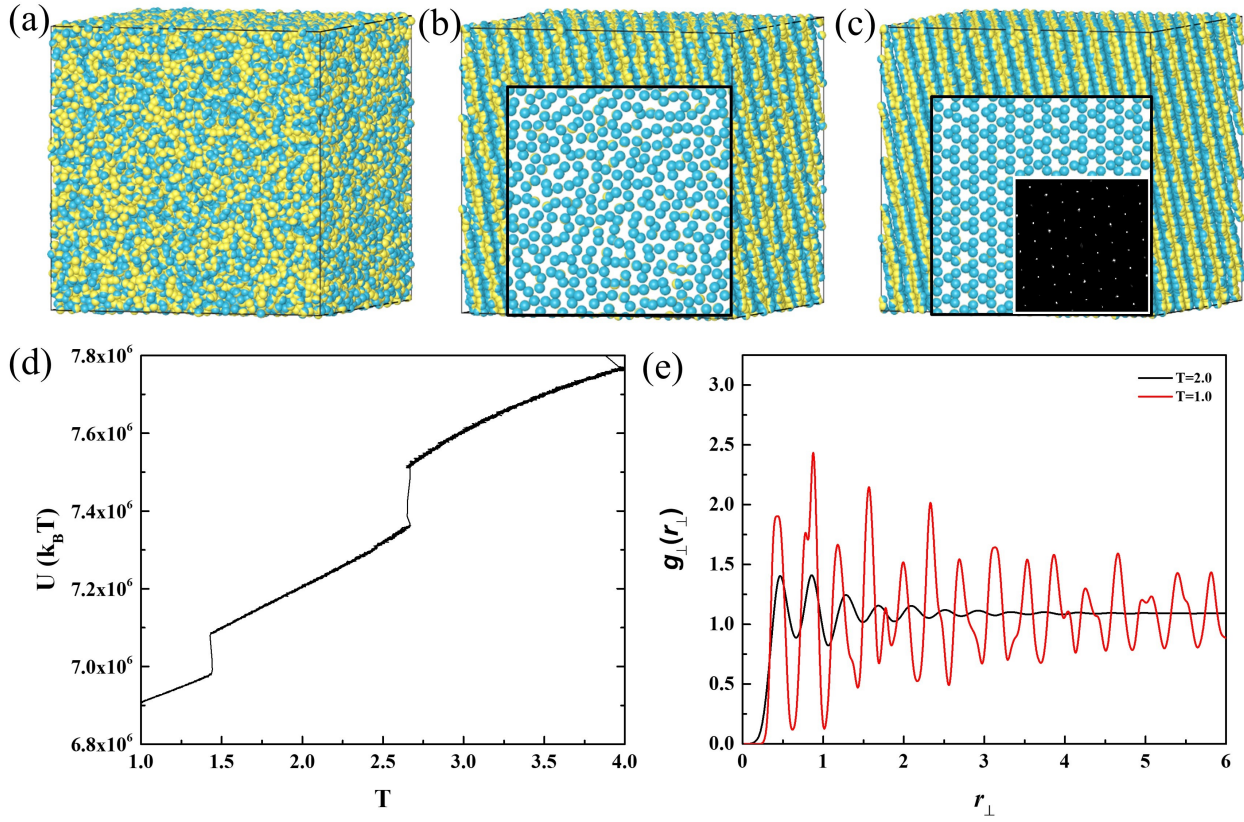


Figure S7: The influence of temperature on kagome lattice. Typical configurations at (a)  $T = 3.0$ , (b)  $T = 2.0$ , (c)  $T = 1.0$ . (d) Temperature dependence of potential energy. (e) The perpendicular radial distribution function  $g_{\perp}(r_{\perp})$  at different temperature.



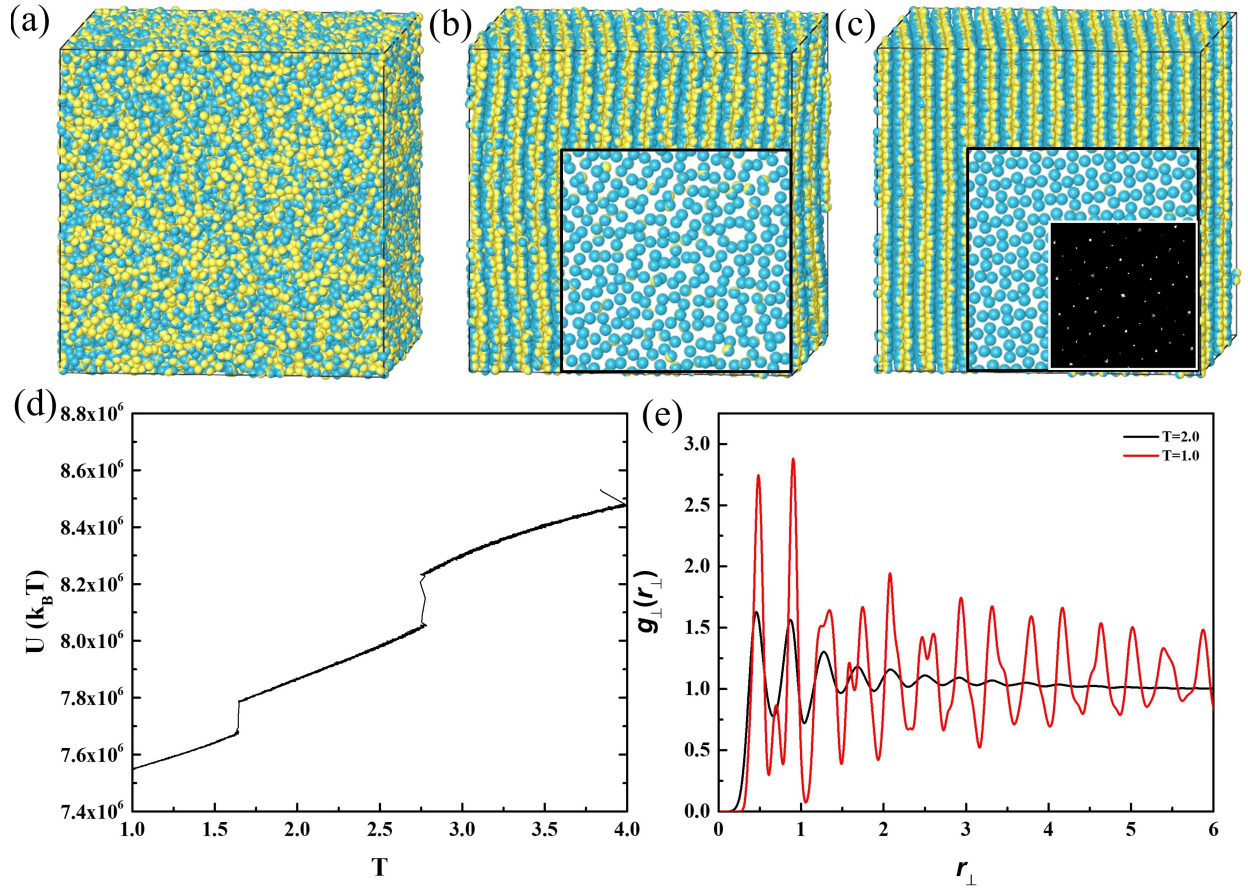


Figure S8: The influence of temperature on  $\sigma$  phase. Typical configurations at (a)  $T = 3.0$ , (b)  $T = 2.0$ , (c)  $T = 1.0$ . (d) Temperature dependence of potential energy. (e) The perpendicular radial distribution function  $g_{\perp}(r_{\perp})$  at different temperature.



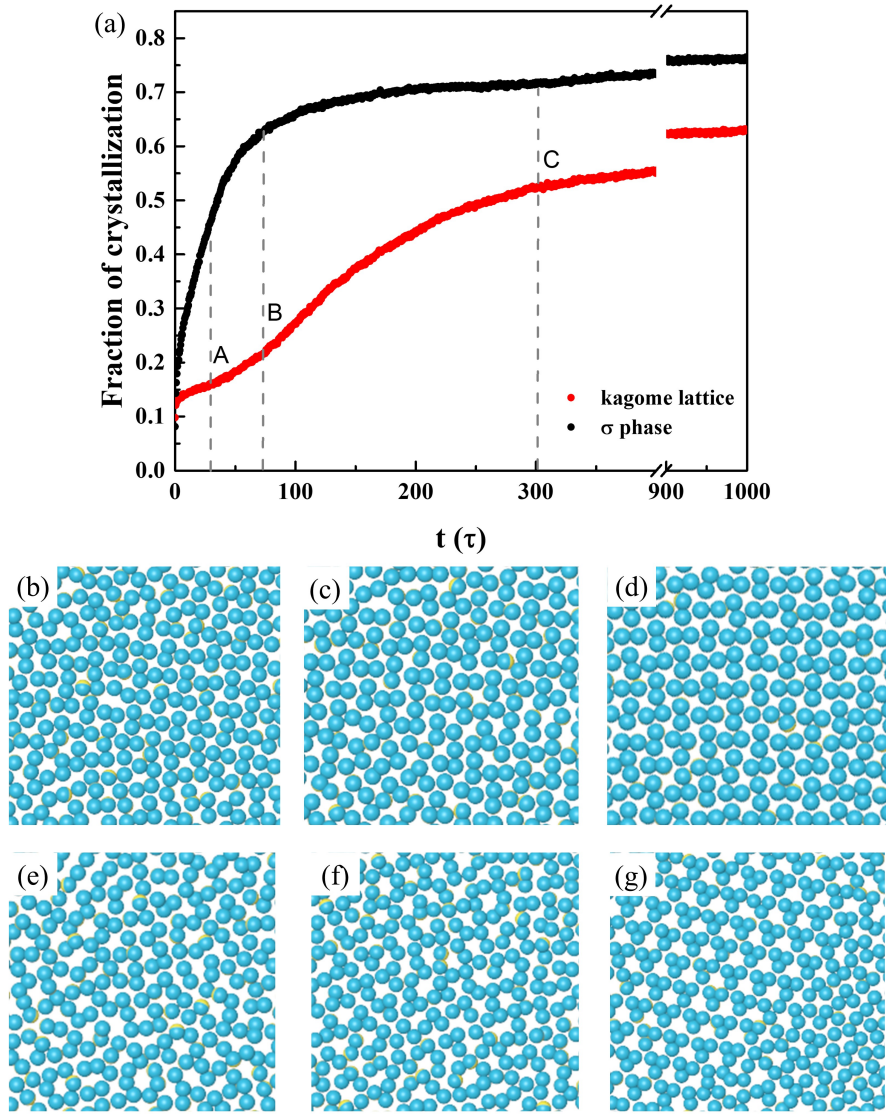


Figure S9: Time evolution of the crystallization fraction. (a) The black lines represents the time evolution of the fraction of  $\sigma$ -like particles, the red lines represents the time evolution of the fraction of kagome-like particles. (b)-(d) Typical snapshots at the simulation times marked by A, B, C of  $\sigma$  phase. (e)-(g) Typical snapshots at the simulation times marked by A, B, C of kagome lattice.

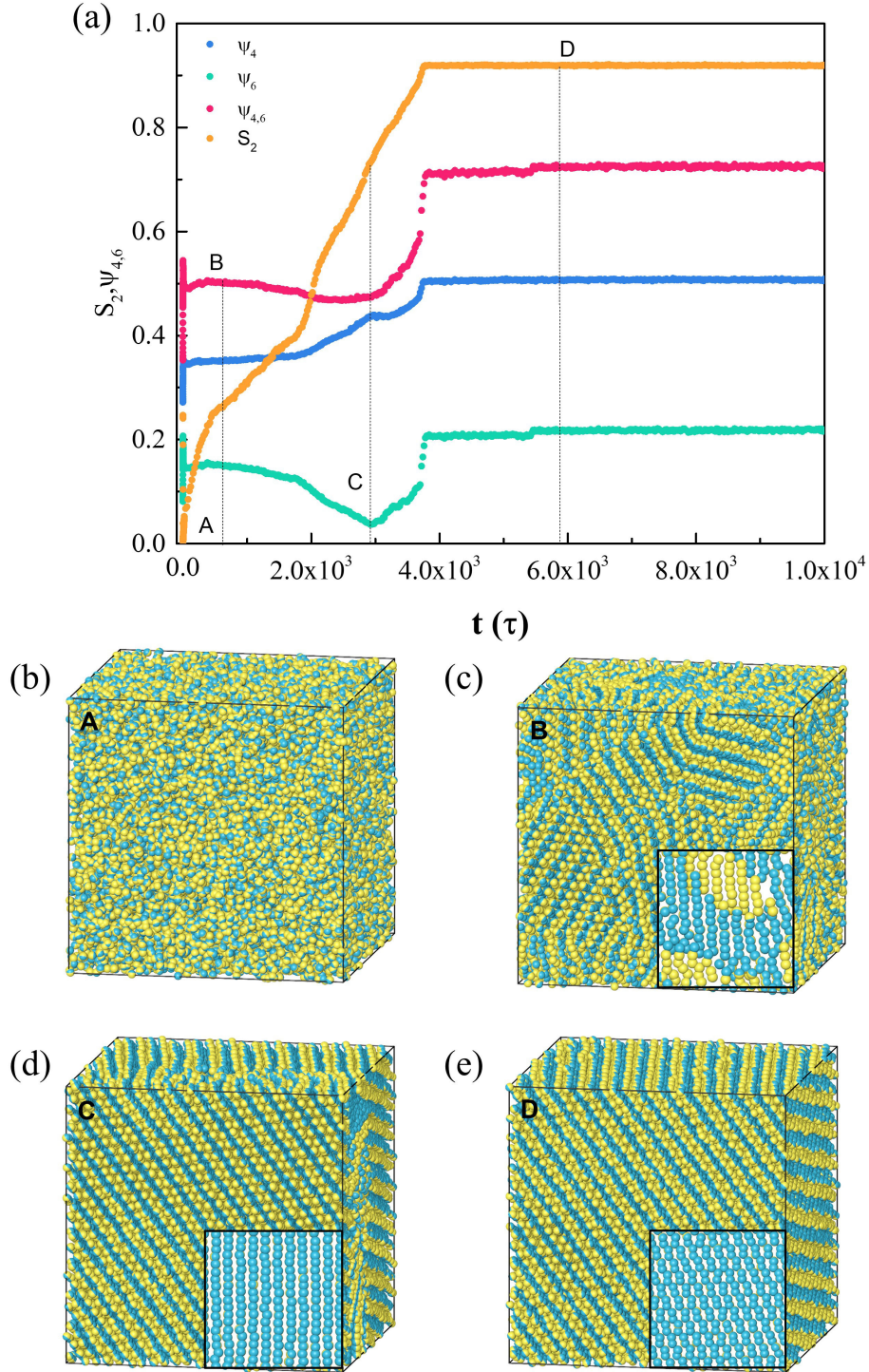


Figure S10: Kinetics of the formation of stretched honeycomb lattice. (a) Time evolution of order parameters. Yellow line represents the orientational order parameter  $S_2$ . Blue, green and red lines represent bond orientational order parameter  $\Psi_4$ ,  $\Psi_6$ ,  $\Psi_{4,6}$ , respectively. (b)-(e) Typical snapshots at the simulation times marked A-D in (a). System of soft Janus particles with  $\beta = 130^\circ$  is chosen to show the formation kinetics.

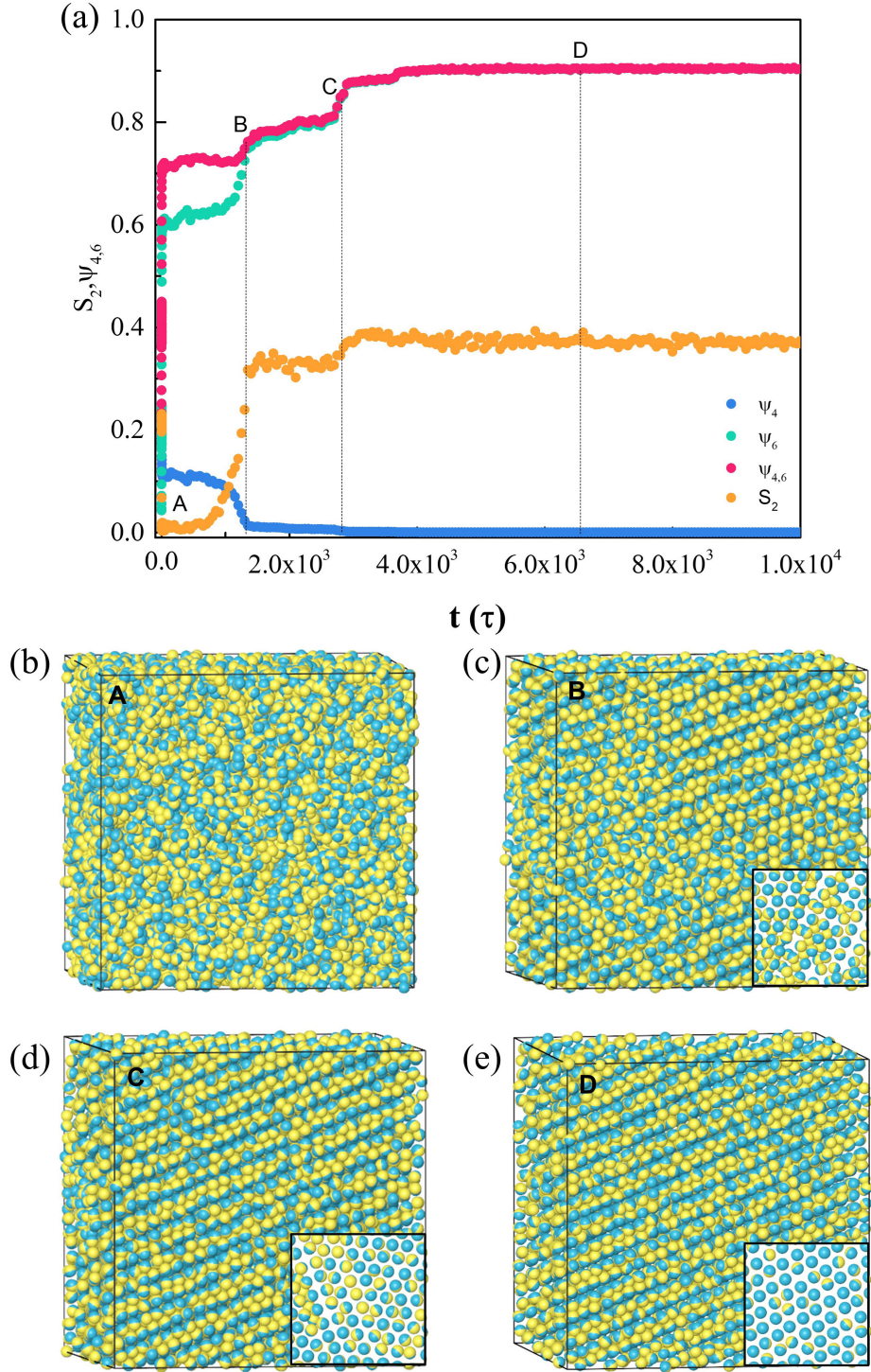


Figure S11: Kinetics of the formation of triangular lattice. (a) Time evolution of order parameters. Yellow line represents the orientational order parameter  $S_2$ . Blue, green and red lines represent bond orientational order parameter  $\Psi_4$ ,  $\Psi_6$ ,  $\Psi_{4,6}$ , respectively. (b)-(e) Typical snapshots at the simulation times marked A-D in (a). System of soft Janus particles with  $\beta = 130^\circ$  is chosen to show the formation kinetics.



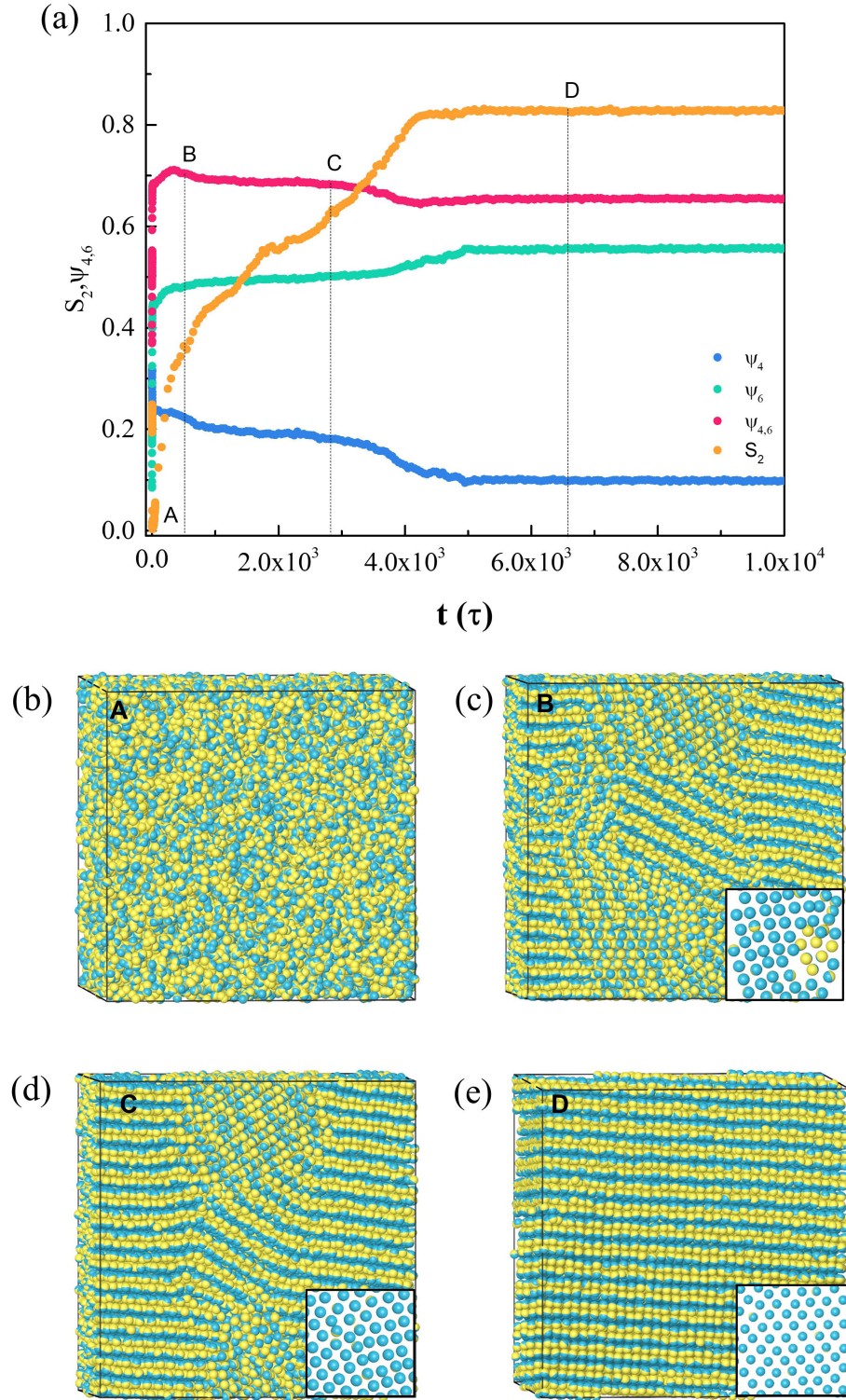


Figure S12: Kinetics of the formation of rhombus lattice. (a) Time evolution of order parameters. Yellow line represents the orientational order parameter  $S_2$ . Blue, green and red lines represent bond orientational order parameter  $\Psi_4$ ,  $\Psi_6$ ,  $\Psi_{4,6}$ , respectively. (b)-(e) Typical snapshots at the simulation times marked A-D in (a). System of soft Janus particles with  $\beta = 130^\circ$  is chosen to show the formation kinetics.

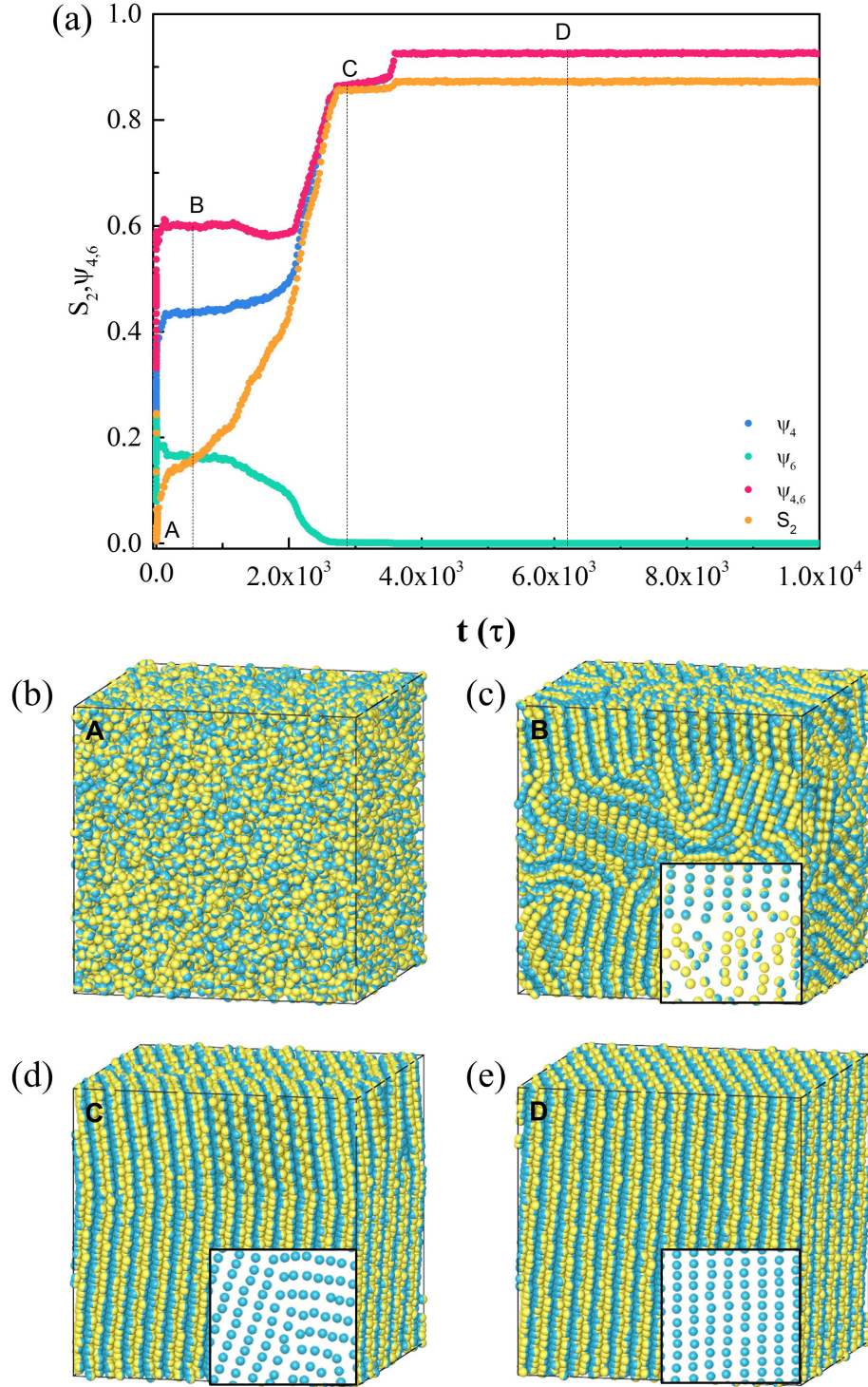


Figure S13: Kinetics of the formation of rectangular lattice. (a) Time evolution of order parameters. Yellow line represents the orientational order parameter  $S_2$ . Blue, green and red lines represent bond orientational order parameter  $\Psi_4$ ,  $\Psi_6$ ,  $\Psi_{4,6}$ , respectively. (b)-(e) Typical snapshots at the simulation times marked A-D in (a). System of soft Janus particles with  $\beta = 130^\circ$  is chosen to show the formation kinetics.



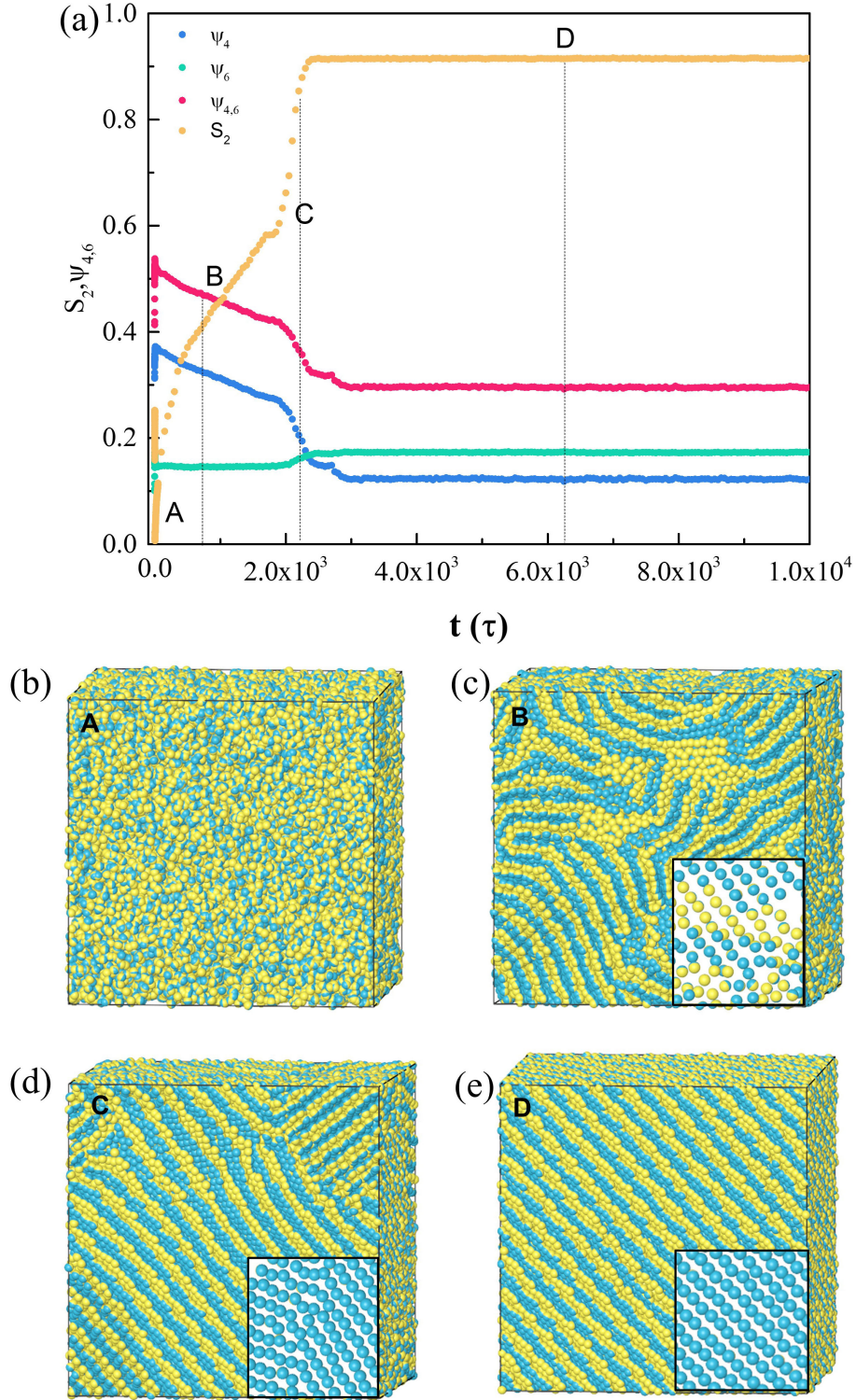


Figure S14: Kinetics of the formation of stripe lattice. (a) Time evolution of order parameters. Yellow line represents the orientational order parameter  $S_2$ . Blue, green and red lines represent bond orientational order parameter  $\Psi_4$ ,  $\Psi_6$ ,  $\Psi_{4,6}$ , respectively. (b)-(e) Typical snapshots at the simulation times marked A-D in (a). System of soft Janus particles with  $\beta = 130^\circ$  is chosen to show the formation kinetics.

## References

- (1) F. Sciortino, A. Giacometti and G. Pastore, *Phys. Rev. Lett.*, 2009, **103**, 237801.